Experimental Comparison of Spark and Jet Ignition Engine Operation with Ammonia/Hydrogen Co-fuelling

A Ambalakatte, S Geng, A Cairns, A LaRocca
University of Nottingham

A Harington, J Hall, M Bassett
MAHLE Powertrain Ltd.

Abstract

Ammonia (NH_3) is emerging as a potential fuel for longer range decarbonised heavy transport, predominantly due to favourable characteristics as an effective hydrogen carrier. This is despite generally unfavourable combustion and toxicity attributes, restricting end use to applications where robust health and safety protocols can always be upheld. In the currently reported work a spark ignited thermodynamic single cylinder research engine was upgraded to include gaseous ammonia and hydrogen port injection fueling, with the aim of understanding maximum viable ammonia substitution ratios across the speed-load operating map. The work was conducted under stoichiometric conditions with the spark timing re-optimised for maximum brake torque at all stable logged sites. The experiments included industry standard measurements of combustion, performance and engine-out emissions. It was found possible to run the engine on pure ammonia at low engine speeds at low to moderate engine loads in a fully warmed up state. When progressively dropping down below this threshold load limit, an increasing amount of hydrogen co-fueling was required to avoid unstable combustion. All metrics of combustion, efficiency and emissions tend to improve when moving upwards from the threshold load line. A maximum net indicated efficiency of 40% was achieved at 1800rpm 16bar IMEPn, with efficiency tending to increase with speed and load. Furthermore comparing spark ignition with active and passive jet ignition (with the former involving direct injection of hydrogen into the pre-chamber only and the main chamber port fueled with ammonia), at different loads it was found that active systems can significantly improve early burn phase and reduce engine-out NOx compared to passive jet ignition and SI. While both Jet ignition systems required supplementary hydrogen, it accounted for ~1% (active) of the total fuel energy at high loads increasing with reduction in engine load.

Introduction

The transportation sector is going through a renaissance in response to increasing pressures from global governments and society to reduce emissions of greenhouse gases and other pollutants resulting from the use of fossil fuels for power. While electrification is often the preferred solution to tackle this challenge, relative immaturity of battery technology combined with associated lack of energy density make full electric propulsion unsuitable for heavy transport applications such as marine, off-road and freight rail.

Ammonia has gained significant interest in recent years, both as a decarbonised energy vector and efficient hydrogen carrier. Volumetrically, liquid ammonia can store ~45% more hydrogen than liquid hydrogen. Furthermore, ammonia can be inexpensively stored as liquid (at -33^0C at 0.1 MPa or 0.86 MPa at 15^0C) and conveniently transported. Such promising characteristics of ammonia have led many researchers to believe ammonia could become a key fuel for heavy transport provided key challenges around slow combustion and emissions control can be overcome [1,2].

The concept of using ammonia as a fuel in internal combustion engines can be traced back nearly a century, where it was used to run buses in Belgium during the 2nd World War [3]. This was followed by extensive research in the mid-1960s, where experiments were carried out in both compression ignition and spark ignition engines. Due to the high auto ignition temperature of ammonia, pure ammonia operation in Compression Ignition engines (CI) is only possible with very high compression ratio (e.g. ~35:1) [4]. As a result, most studies in CI engines focus on “dual fuel” operation, where a pre-mixed ammonia-air mixture is ignited by a pilot fuel of low auto ignition temperature and favourable cetane rating.

The dual fuel approach has been extensively researched with various fuels including diesel, DME, kerosene and amyl-nitrate [5–12]. However, the added complexity of an additional fuel circuit, coupled with difficulties in operating the engines under throttled conditions and high carbon content of the pilot fuel, makes this solution less attractive compared to spark ignition engines. Compared to compression ignition, pure ammonia operation can be achieved in spark ignition engines at considerably lower compression ratios as reported by Starkman et al. as early as the 1960s [13]. Pearsall et al. [10] investigated the operation with ammonia in both types of engines and recommended a high compression ratio (e.g. 12-16) spark ignition engine as an ideal solution for best compromise between efficiency and pollutant emissions.

While better than compression ignition, the relatively poor premixed combustion characteristics of ammonia (see Table 1) makes it challenging to operate a spark ignition engine with pure ammonia at low loads. However, several strategies can be considered such as increasing the effective compression ratio, supercharging (potentially without inter-cooling), and co-fuelling with a faster burning sustainable fuel (s). Of these solutions, co-fuelling with hydrogen has been more extensively studied [14–18] due to excellent combustion characteristics combined with the potential ability to produce the hydrogen onboard via ammonia “cracking” [19,20].

Morch et al. [21] investigated the combustion of ammonia at different hydrogen substitution levels and concluded that ~10% volume substitution yielded maximum thermal efficiency. Further to this, Firgo et al. [22] investigated ammonia-hydrogen co-fuelling at various speed/load conditions and concluded that combustion improvement from hydrogen enrichment had reduced impact on engine speed extension compared to engine load. They further calculated the minimum amount of hydrogen energy required for

stable combustion to be roughly ~7% for full load and ~11% for part load conditions. These researchers also investigated the feasibility of using exhaust gas heat to crack ammonia on board and confirmed that hydrogen can be produced via the solution, however, the higher combustion temperatures required for the cracker resulted in significantly higher NOx emissions [23]. Recently investigations conducted by Lhuillier et al. [24] and Mounaïm-Rousselle et al. [25] in modern spark ignition engines also concluded that the combustion of ammonia can be greatly improved by small amounts of hydrogen (~10% vol.), allowing the engine to operate at various loads and engine speeds ranging from 650rpm to 2000rpm.

Table 1 Combustion Characteristics of Ammonia, Hydrogen and Gasoline [26–30]

Species	Hydrogen	Ammonia	Gasoline
Chemical Formula	H_2	NH_3	$C_nH1.87_n$
LHV [MJ/kg]	120	18.8	44.5
Laminar Burning Velocity @ λ=1 and ambient conditions [m/s]	3.51	0.07	0.58
Auto-ignition Temperature [K]	773-850	930	503
Research Octane Number	>100	130	90-98
Flammability Limit in Air [vol. %]	4.7-75	15-28	0.6-8
Quench Distance [mm]	0.9	7	1.98
Absolute Minimum Ignition Energy [mJ]	0.02	8	0.1

The use of hydrogen in prechambers was pioneered by Watson et al. in the late 90s [31–34], however there is a lack of studies investigating the application of hydrogen assisted pre-chambers for ammonia combustion. While this topic is garnering significant interest in recent years, most of the published work has focused on numerical or computational simulations with most experimental works conducted in constant volume combustion chambers[35]. Cui et al. [36] studied the effects of pre-chamber geometry on ammonia combustion and found a larger geometry pre-chamber with larger orifices tend to develop better combustion characteristics which they accredited to the lower heat dissipation inside the pre-chamber. Following this Zhang et al. [37] conducted studies visualising the combustion as well as the impact of methane addition on ammonia/air mixtures, they found that 10% addition of methane enhanced the combustion, while further increase in methane concentration had negligible impact on the combustion for both jet ignition and direction injection systems.

The currently reported work involves experimental research using a modern spark ignited thermodynamic single cylinder engine operating on ammonia and hydrogen over a range of speed and load points, with the aim of improving understanding of the maximum viable substitution of ammonia across the operating map. The goal was to undertake a baseline analysis in a high performance gasoline engine equipped with a modern combustion chamber layout and durable high energy ignition system designed for highly downsized spark ignition engines (e.g. >30bar IMEP). Furthermore, the paper also includes an initial comparison between Spark ignition (SI), and variations of MAHLE Powertrain's pre-chamber Jet Ignition systems (MJI) namely Passive Jet Ignition (Passive MJI) and Active Jet Ignition (Active MJI) combustion with ammonia-hydrogen mixtures at a constant speed of 1400rpm and engine load varying from 4 bar IMEPn to 12 bar IMEPn.

Experimental setup

Engine hardware

Even though the intended applications of ammonia is in heavy duty engines, the reported experiments were conducted in an automotive grade single cylinder derivative of the Mahle "DI-3" engine[38]. This hardware has a highly optimised pre-chamber systems ensuring which minimises/eliminates many of the inherent challenges of pre-chamber systems such as scavenging, cooling etc. all of which have negative impact on the combustion. However, the use of ammonia in this hardware had its own set of challenges such as limiting the compression ratio to 12 and potential quenching of ammonia flame inside the pre-chamber owing to its small volume.

The engine was equipped with a central spark plug and side mounted gasoline direct injector located under the intake valves for delivering standard pump grade E10. Ammonia was delivered at the port via an upgraded manifold using a prototype Clean Air Power port fuel injector. The engine was also equipped with hydraulic fully independent variable valve timing to enable optimisation of valve timing and overlap. Set out in Table 2 are the key characteristics of the engine.

Table 2 Engine hardware specifications

Parameters	Value	
Engine Type	Four Stroke Single Cylinder Spark Ignition	
Displaced Volume	400 cc	
Stroke	73.9 mm	
Bore	83 mm	
Compression Ratio	12.39	
Number of Valves	4	
Valvetrain	Dual Independent Variable Valve Timing (40°CA Cam Phasing)	
Fuel Injection Configuration	Gasoline E10	Side DI
	Hydrogen	PFI (SI and Passive MJI) Pre-chamber DI (Active MJI)
	Ammonia	PFI
Cylinder Head Geometry	Pent Roof (High Tumble Port)	
Piston Geometry	Pent-Roof with cut-outs for valves	
Ignition Coil	Single Fire Coil, 100mJ, 30kV	
Max Power	40 kW (Gasoline)	
Max Torque	96 Nm (Gasoline)	
Max In-Cylinder Pressure	120 bar	
Max Speed	5000 rpm	
Boost System	External Compressor (Max 4barA)	
Control System	MAHLE Flexible ECU	
Control Software	ETAS INCA	

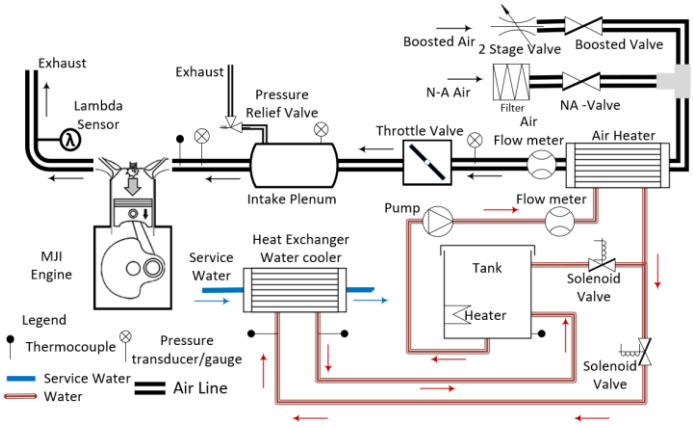

Figure 1 Schematic of the engine test rig

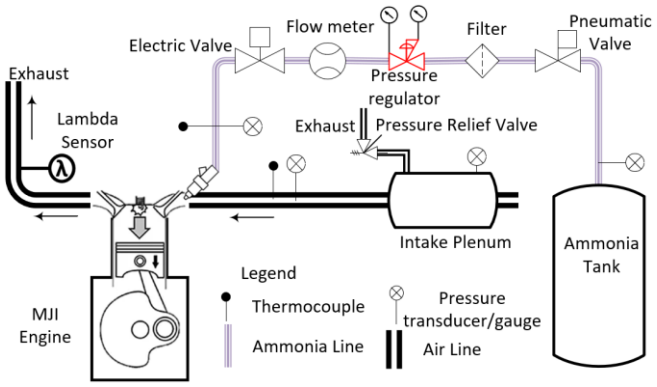

Figure 2 Schematic of the engine NH_3 fuel supply line

The ammonia was supplied to the engine in gaseous phase using a dedicated port injector supplied by Clean Air Power (CAP). The ammonia was stored in liquid vapour equilibrium via a drum, with the pressure differential between the intake manifold and vapour pressure inside the drum used to drive the supply of ammonia to the engine. The flowrate of ammonia was measured using a Coriolis flowmeter procured from micro-motion (maximum flow rate error of 1% at the minimum flow rates reported). Electrically controlled safety valves and nitrogen-based purging were added to the supply line to isolate the ammonia supply in the case of an emergency. For the gasoline supply, an AVL 735 fuel balance unit was used to measure the gasoline (E10) flowrate and condition the gasoline temperature (20°C set point) before being fed to a high-pressure fuel pump at constant supply pressure via a fuel regulator.

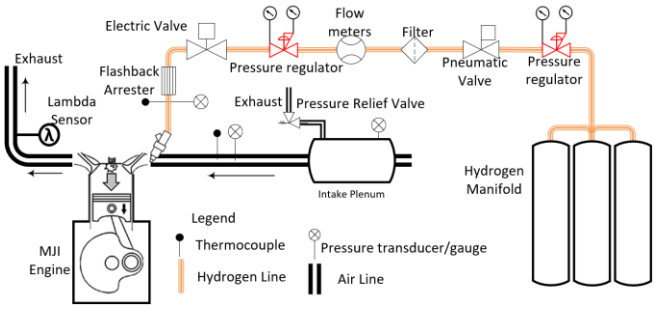

Figure 3 Schematic of Hydrogen Supply system

The schematic of the hydrogen fuel line is given in figure 3, similar to ammonia, hydrogen too was delivered to the engine using dedicated port fuel injectors from Clean Air Power from a hydrogen manifold where the hydrogen was stored at 172 bar pressure. The pressure was regulated down to 10 bar at the injector using two pressure regulators, with the first of these reducing the hydrogen supply pressure from the manifold to 50bar which ensured accurate reading (errors within 1%) by the Coriolis flowmeters from Alicat. The second regulator reduces the pressure further for the Port Fuel Injector (PFI) (max 20bar), in addition to the regulators, safety valves and flash back arrestors were also added to the hydrogen line to isolate and vent the line in case of an emergency. Further details of the injection timing, feed pressure etc are given in table 4 and discussed later in the report. For both SI and PFI tests, hydrogen was injected during the suction stroke to ensure low residence time in the intake manifold as well as prevent hydrogen flowing into the exhaust from the cylinder scavenging. In case of Active JI tests the direct injection (DI) was initiated in the compression stroke to minimize the diffusion of injected hydrogen into the main chamber.

Cylinder pressure was measured using a Kistler 6045-B piezo electric pressure transducer working through an AVL Micro-FEM amplifier, fully calibrated to industry standards via a dead weight tester. The intake and exhaust were measured using Kistler's 4045A and 4011 piezo resistive transducers. The engine-out emissions were measured using a series of dedicated analysers from the Signal group, in addition to industry standard emissions (NOx, CO_2, CO, THC and O_2), ammonia "slip" emissions (unburned NH_3 in the exhaust) were also measured based on a new unit, with details of the emission analysers given in Table 3. All measurements were recorded and processed using a bespoke National Instruments data acquisition system. The data from the pressure transducers was recorded at a resolution of 0.2 Crank Angle degrees (CAD) using a Hohner 3232 optical encoder, which was synchronised using an AVL capacitive probe. During all testing 300 cycles of pressure data were recorded. Mass fractions burned were evaluated on a qualitative basis using one dimensional heat release analysis. Other "steady state" temperature, pressure and flow measurements were taken at a frequency of 10Hz.

Table 3 Details of Emission Analysers

Equipment	Gas	Operating Principle	Dynamic Range (Volume)	Accuracy / Error(%)
4000 VM	NOx	Chemiluminescence	0-1000 ppm	Better than +1% range or ±0.2 ppm whichever is greater.
8000 M	O2	Dumbbell paramagnetic sensing	0 -5 %, 0 -10 %, 0 -25 %	±0.01 %O2.
S4 Nebula	NH_3	Tuneable Diode laser Spectrometry	1ppm - 10,000 ppm	±2% of FDS
3000 HM	THC	Flame ionisation detector	0-10000 ppm	Better than ±1 % range or ±0.2 ppm whichever is greater.
7000 FM	CO, CO2	Infra-red gas filter correlation technique	100-10000 ppm Or 1-100 %	Better than ±1 % of range or ±0.5 ppm whichever is greater.

Test plan

Since practical applications of ammonia are expected to be in low-to-medium speed heavy duty engines, the test points were selected to cover typical peak power speed ratings of similar engines. The tests were conducted at 1000, 1400 and 1800rpm with the engine load varied from 4 to 12bar net Indicated Mean Effective Pressure (IMEPn). The aim of the tests was to determine the pure ammonia speed-load map and impact upon combustion, performance, fuel economy and emissions with and without co-fuelling. The co-fuelling required was evaluated by undertaking ammonia "displacement sweeps"; with the engine first fired using pure E10 and NH_3 progressively added until an upturn in combustion stability occurred (with repeat logs around this upturn to establish

the maximum possible NH_3 substitution and the upper limit set to a coefficient of variation in IMEP of >3%). All logs were obtained under stoichiometric conditions with the spark timing set to maximum brake torque. In early work it was proposed that slightly rich running might aid NH_3 displacement (due to slightly higher laminar burning velocity) but this was not found to be the case; with the engine misfiring more easily when attempting to operate slightly richer when at the substitution ratio limit due to the relatively low relative air-to-fuel ratio of NH_3 and significant reduction in the ratio of specific heats "over-ruling" relatively small increases in laminar burning velocity when slightly rich. Such effects were previously indicated in the chemical modelling work by Kobayashi et al. [39].

The engine settings used for the tests are set out in Table 4. In addition to these settings the valve timing was fixed for the tests. However, the overlap was adjusted from 37 Crank Angle Degrees (CAD) to 24 CAD for the 1000rpm tests as the slow speed combined with high boost pressure resulted in the significant ammonia slip due to high apparent cylinder scavenging at this speed.

Table 4 Engine settings for substitution tests

Settings	Values
Operating Temperature (Coolant & Oil)	95 ^{0}C
Spark Timing	Maximum Brake Torque (MBT)
Air-fuel Equivalence ratio	1
E10 Injection Start angle	310 CAD BTDCf
Ammonia Injection End angle	400 CAD BTDCf
PFI Hydrogen Injection Start angle	340 CAD BTDCf
Active Hydrogen injection start angle	140 CAD BTDCf
Inlet air temperature	45^{0}C
Ammonia rail pressure	3-5 barG
Ammonia Feed Temperature	27 ^{0}C -30 ^{0}C
Hydrogen Feed Pressure	28 barG (Active DI injector) 2 barG (PFI)
Hydrogen Feed Temperature	27 ^{0}C -30 ^{0}C

Results

Maximum displacement of ammonia (Energy Fraction)

The results of the maximum displacement of ammonia expressed as energy fraction of the fuel consumed at various test points are shown in Figure 4.

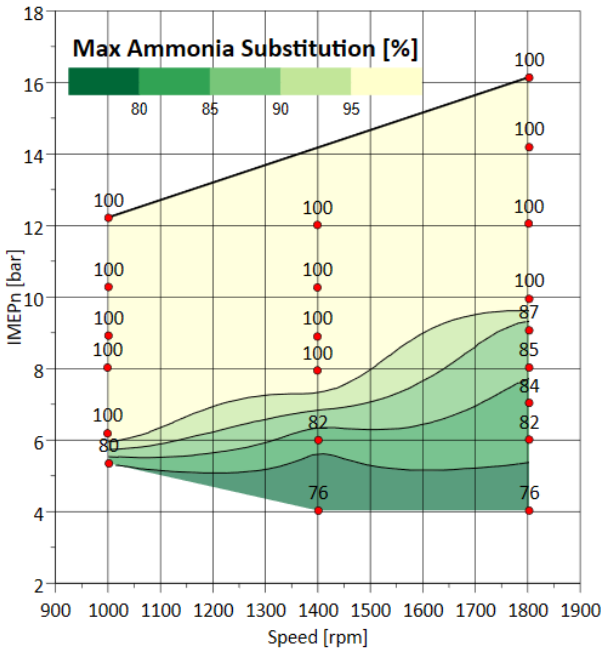

Figure 4 Maximum substitution of ammonia achieved at different load points (λ=1, MBT spark timing)

As seen from the figure 4, the engine could be operated with pure ammonia at moderate to high loads across the test region. The 100% substitution isoline follows a near-linear pattern, with the threshold load required to operate on pure ammonia increasing by 2bar IMEPn for an increase of 400rpm in engine speed. This direct relation of threshold engine load and engine speed was also observed by Mounaïm-Rousselle et al. [25] in their work on ammonia spark ignition engines. This trend is despite increasing gas temperatures and turbulence at higher speeds and illustrates the dominance in lower speed providing more time for combustion to occur despite the fact the in-cylinder and exhaust gas temperatures usually increase with engine speed (for a given load). The impact of increasing in-cylinder turbulence with higher speed remains unknown and will be qualified in future work, however tests conducted by Silva et al [40] indicate a similar trend for both temperature and turbulence, where enhancement of both with speed have negligible impact on the combustion of ammonia.

As the load decreases below the threshold loads for 100% percent operation, hydrogen enrichment was required to operate the engine stably. However, the maximum substitutions achieved in these tests were limited by the hydrogen injector hardware rather than combustion. The minimum flow rate of the injector was higher than the required flow rate for combustion limited operation, as a result all the enrichment points were operated at the minimum injection time (~0.1 ms) and a feed pressure of ~2barG (limited by the check valves in the fuel line) as illustrated in Figures 5 and 6.

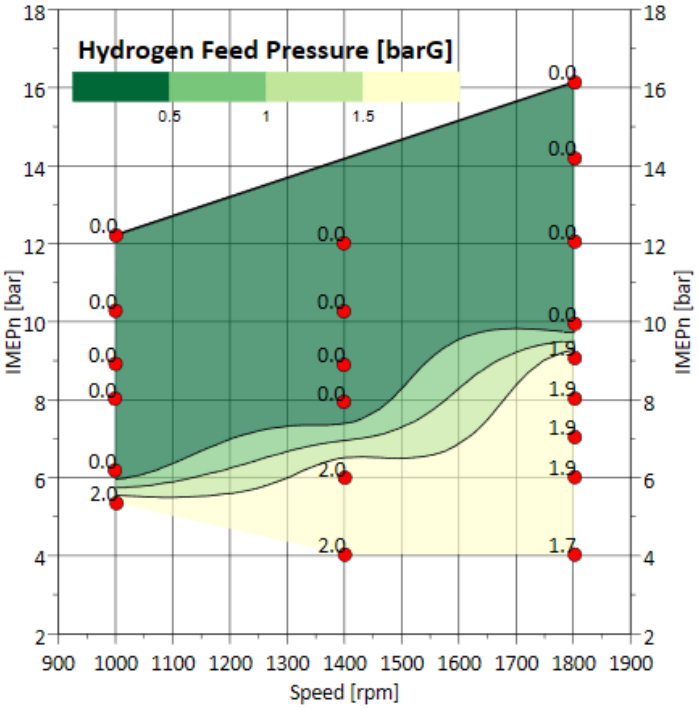

Figure 5 Hydrogen feed pressure at various test points

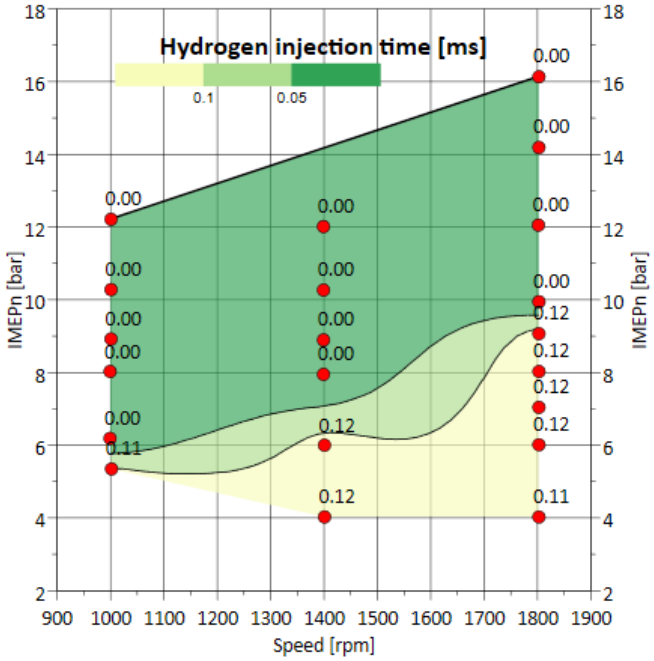

Figure 6 Injection time of the hydrogen injector for various test points

General trends of ammonia + hydrogen operation in an SI engine

Combustion

Figures 7 and 8 show the spark timing required to achieve MBT and the corresponding stability of the engine at the tested points. Examining both figures, the transition from NH_3+H_2 to pure NH_3 is evident as the values peaks at the threshold load point for each tested engine speed. The engine operation improves considerably as the test points move away from the threshold load.

The addition of hydrogen below the threshold load improves the combustion and stability drastically, as suggested by the spark timing for MBT improving as much as 10 CAD. Similarly, the stability drops below 1% CoV compared to the 3% at the threshold load. Both data sets suggest the amount of hydrogen needed operate the engine at its combustion limit should be significantly lower than the amount of hydrogen added at these points. Furthermore, analysing the pure ammonia operation, both stability and spark advance needed to achieve MBT, improves as the load increases from the threshold load line and with reduction in engine speed. While the improvements in spark timing is gradual, the engine operation becomes notably stable beyond 4bar IMEPn from the threshold load at all engine speeds.

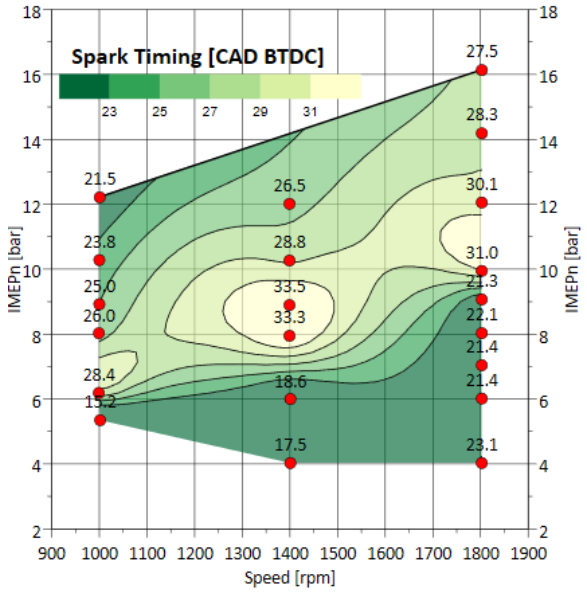

Figure 7 Spark timing required for MBT engine operation at the test points

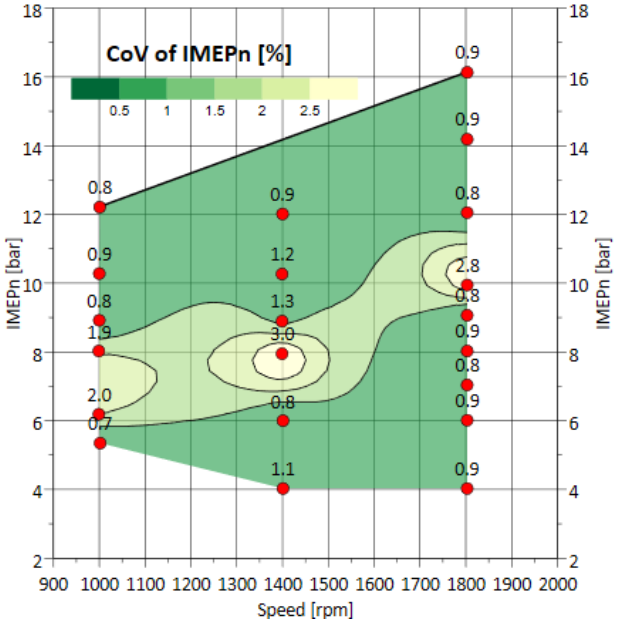

Figure 8 CoV of IMEPn of engine operation at the test points

The mass fraction burned at the various test points is shown in Figure 9, where the “flame development phase” (0-10% MFB) followed a similar trend to the spark timing. However, the “combustion phase” (10-90% MFB) given in Figure 10 shows relatively smaller variation for all the test points. Moreover, in the pure ammonia operation region, the flame development phase was identical to the combustion phase at low speeds and becomes larger than the combustion phase as speed increased. In other words, nearly 50% or more of the total combustion duration encompasses the flame development phase. The lack of variation in the combustion phase with speed could be a direct result of increased turbulence enabled by a high tumble head used in the study (to be confirmed in future optical and CFD analysis work).

The impact of hydrogen enrichment is more noticeable in the flame development phase, where the duration decreases by nearly 50%, and remains smaller than the combustion phase compared to the pure ammonia operation. Furthermore, the values of flame development phase remained identical for all points in a given engine speed suggesting a higher correlation with the mass of hydrogen than substitution ratio between ammonia and hydrogen.

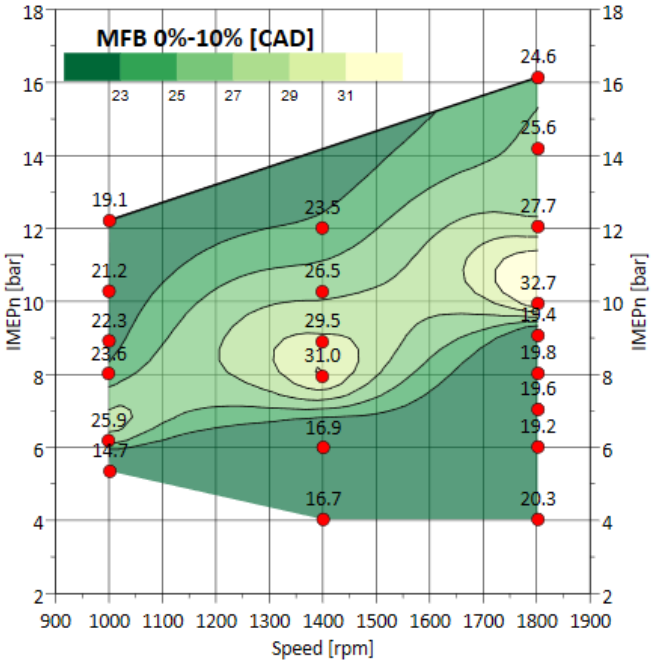

Figure 9 Variation of combustion metric 0%-10% MFB at various test points.

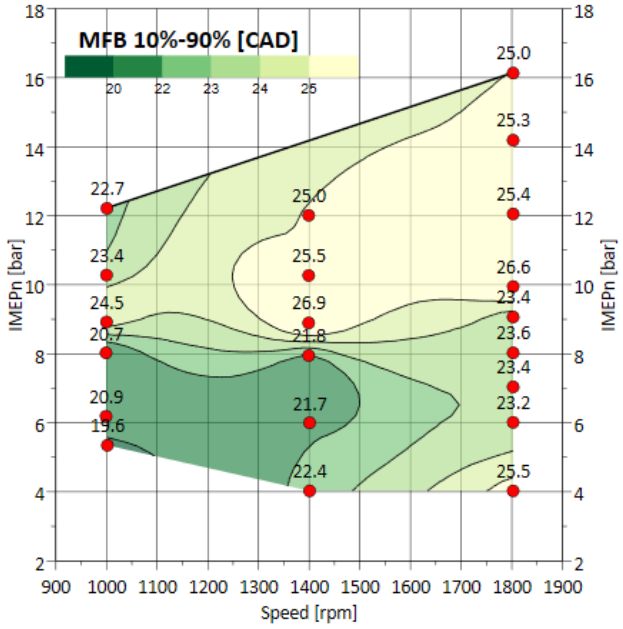

Figure 10 Variation of 10%-90% MFB for the Various test points

The CA50 of ammonia-hydrogen tests and pure E10 operation are given in figure 11 and 12 respectively. As seen from the figures, the anti-knock characteristics of ammonia enables optimal operation with MBT spark timing (CA 50 at 8 CAD ATDC). In comparison, pure E10 operation is knock limited beyond 6 bar IMEPn requiring a retarded spark timing defined as Borderline Detonation-1(BLD-1) to prevent knocking and healthy operation of the engine. BLD-1 spark timing negatively impacts the efficiency which is discussed in the next section.

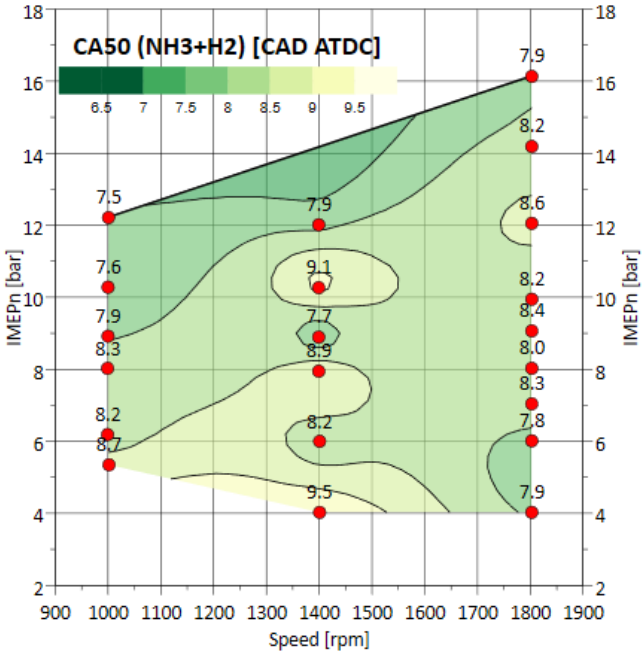

Figure 11 CA50 for ammonia-hydrogen co-fueling at various test points

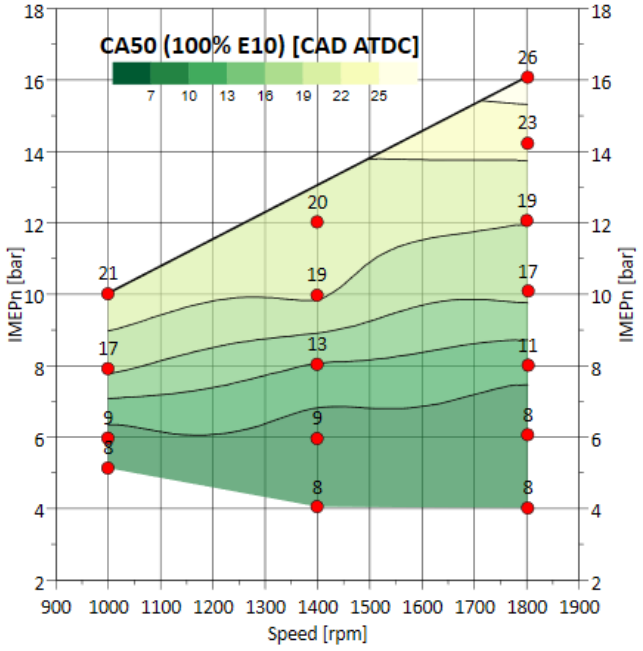

Figure 12 CA50 for pure E10 operation at various test points

Efficiency

The variation in net Indicated Thermal Efficiency (ITE) in the test region for NH_3+H_2 and pure E10 operation is set out in Figures 13 and 14 respectively. Operating the engine on NH_3 and H_2 is considerably more efficient (~14%) than E10 in the test region due to the following reasons.

- **Kock resistance of ammonia** allows the engine to be operated with optimal spark timing (MBT) as opposed to the knock limited spark timing in (BLD-1) in case of pure E10. BLD-1 timing forces most of the combustion to occur during the power stroke limiting the conversion of useful energy as work thereby reducing the efficiency.
- **Low air-fuel ratio** in case of ammonia (6 vs 13.8 for E10) allows the wide open throttle operation of engine at low loads reducing the pumping losses in the tests region.
- **Slower heat release of** ammonia combustion reduces the heat losses to cylinder walls ensuring more of the released energy

is converted to useful work. E10 on contrast has a higher rate of heat release which is lost as heat resulting in the same efficiency for a given speed regardless of the load.

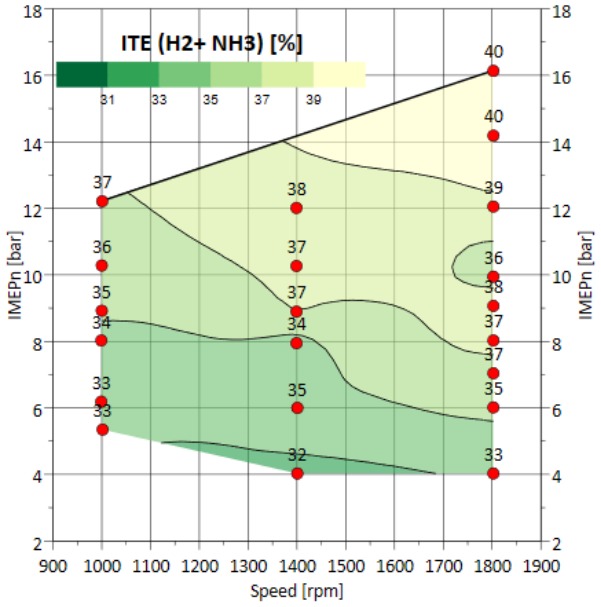

Figure 13 ITE achieved with Ammonia & Hydrogen fuel mix at various test points

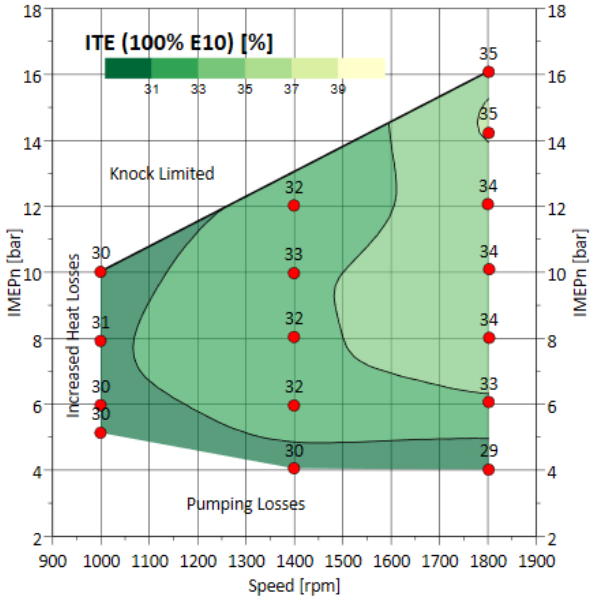

Figure 14 ITE achieved on 100% E10 operation

Examining the variation of ITE for NH_3+H_2 operation, the efficiency improves with increase in speed and load (with the exception of the threshold load points where a drop in efficiency is observed). Between speed and load, the impact of load increase is larger than that of engine speed. This variation suggests losses from increased heat rejection, pumping and knock that govern E10 operation in the test region do not directly apply to pure ammonia operation, or these factors have minimal impact on the ITE (potentially related to the ability to achieve MBT across the map).

Furthermore, addition of hydrogen has a positive impact on the efficiency, enabling a higher efficiency operation than the threshold load point at the same engine speed. This could be a result of the significant combustion improvement achieved by the addition of hydrogen.

Emissions

A comparison of NOx emissions with NH_3+H_2 operation and pure E10 operation is given in Figures 15 and 16. Except for the 4 bar IMEPn test points, the NOx emissions from NH_3+H_2 operation is less than 50% of the corresponding value recorded with E10 operation. Within the test region, the NOx emissions remained relatively similar for NH_3+H_2 operation, with the values gradually decreasing with increasing engine load and reducing engine speed. This trend differs completely to pure E10 operation, where NOx emissions increase with engine load and peaks at load where the engine starts to knock (the spark retardation to avoid knock reduces the NOx thereafter). Furthermore, even with significantly advanced spark timing (resulting in higher cylinder temperature), the NOx emissions for pure ammonia operation at higher engine loads were lower than hydrogen enriched operation at low engine loads.

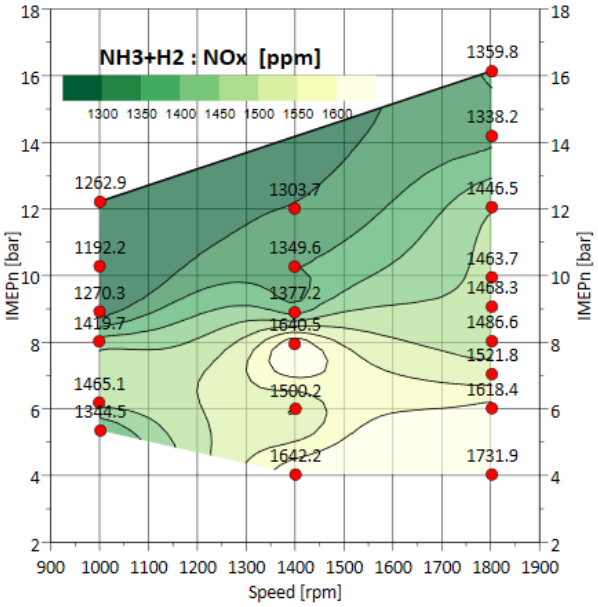

Figure 15 NOx emissions from NH_3+H_2 operation

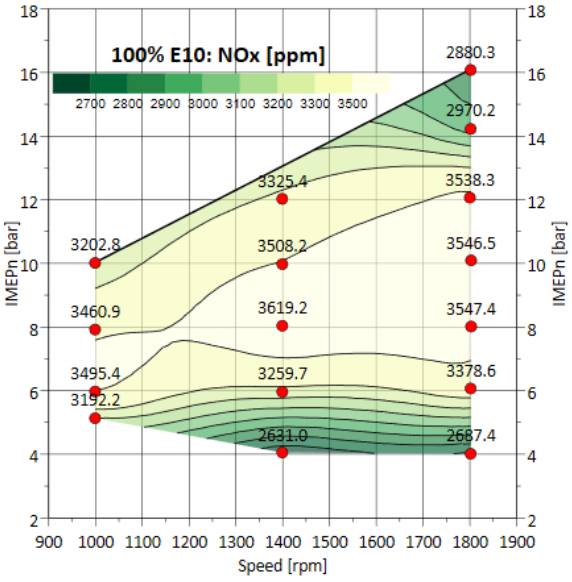

Figure 16 NOx emissions from pure E10 operation

Figure 17 illustrates the unburned ammonia emission data from the test points. Unburned ammonia "slip" peaks near the threshold load from the unstable engine operation in those points. While this improves with engine stability, there is considerable unburned ammonia (> 0.5% vol.) even in stable operating points when operating on pure ammonia.

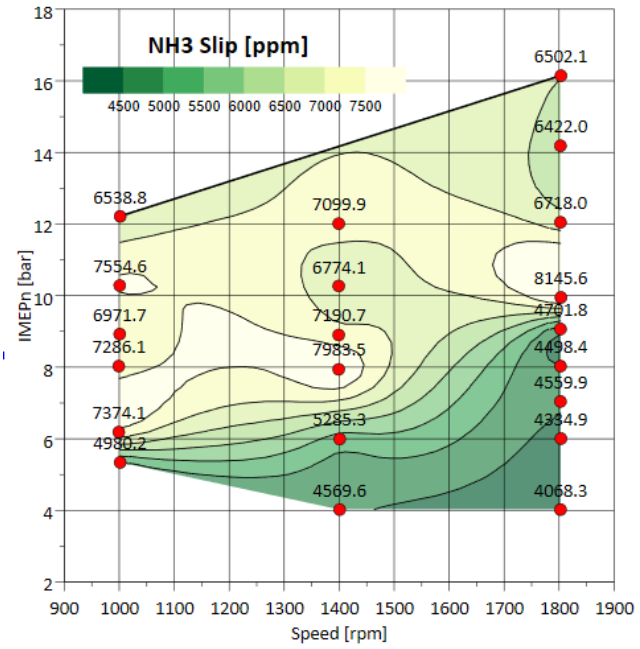

Figure 17 Variation of ammonia slip in the test region

The recorded ammonia slip values are comparable to previous studies published by Lhuillier et al. and Mounaïm-Rousselle et al. [24,41] using "similar" engines and under similar operating conditions (λ=1, MBT). Unburned ammonia in the exhaust drops significantly with the addition of hydrogen, dropping by nearly 50% from the peak values. However, the values remain high even with hydrogen, suggesting the emissions could be due to the incomplete combustion of ammonia trapped in crevice volumes as well as from in-cylinder scavenging, however further investigations are necessary to validate this hypothesis. One of the potential uses of the excessive slip is to clean the NOx in an SCR catalyst, moreover, high exhaust gas temperatures can enable the oxidation of excess ammonia within the catalyst as determined by Girard et al. [42]. However, SCR will require excess oxygen (leaner operation) and the alpha ratio (mass ratio of NH_3 to NOx) is considerably higher than desired values between 1 and 2 for pure ammonia operation, however, the values drops closer to 2 for hydrogen enriched operation. This implies hydrogen enrichment could be a potential "active" solution to overcome ammonia slip.

Comparison of Ammonia – Hydrogen Combustion with SI, Passive MJI and Active MJI

As explained in the previous section, while pure ammonia operation can be achieved at moderate-to-high load operation, some form of fuel enhancement is needed to stably operate the engine at low loads, idling and cold start. However, due to the challenges with storing hydrogen, it is important to maximise the available hydrogen for enhancing the ammonia combustion, this could be achieved by combining hydrogen with a fast-burning combustion system like pre-chamber jet ignition. To understand the viability of such a system, preliminary experiments were conducted with both active and passive variants of MAHLE Powertrain's Jet Ignition systems (MJI), with the main change being the addition of hydrogen.

In a passive MJI system, hydrogen is introduced to the engine via port fuel injection similar to SI systems, while an active MJI system uses a dedicated hydrogen direct injector in the pre-chamber for independent fuelling. The tests were conducted at a constant engine speed of 1400rpm with engine loads varying from 4 bar IMEPn to 12 bar IMEPn (maintaining the same engine settings as given in Table 4). The results from this preliminary test are discussed in the following sections.

Maximum ammonia substitution

The maximum viable ammonia substitution in energy fractions for stable operation at various engine loads is given in Figure 16. However, as mentioned in the previous section, both SI and passive MJI tests were conducted with a larger flow rate hydrogen injector. This resulted in a lower ammonia fraction than required for stable combustion. In the case of the active system, the dedicated injector had a small enough flowrate to achieve a energy fraction of 1% at 11bar IMEPn.

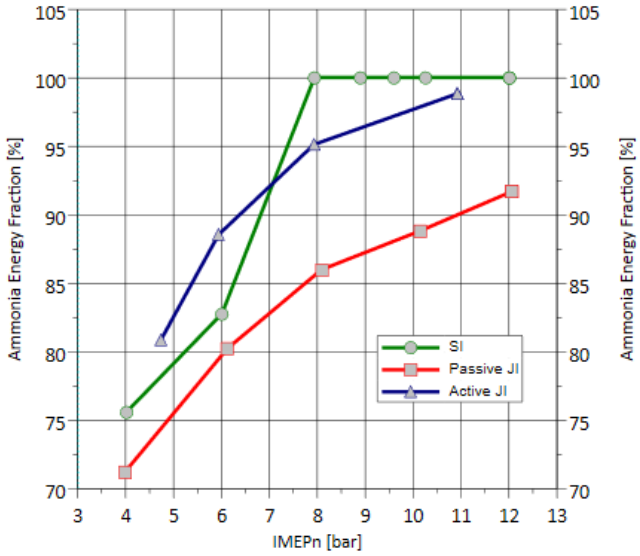

Figure 18 Maximum viable ammonia energy fraction at different load points for the three combustion systems

Of the three combustion systems, passive MJI required more hydrogen compared to the other two solutions. At low loads, the passive MJI system required ~5% higher hydrogen fraction than the SI system which used similar injector hardware. Furthermore, as pure ammonia operation was not possible with MJI systems, the high flowrate of the PFI injector skews the true potential of passive MJI. Concentrating the available hydrogen in the pre-chamber allows the active systems to use significantly less hydrogen than the passive counterpart, especially at low loads. At higher loads (> 8bar IMEPn) less than 5% of hydrogen is required to stably operate the engine, potentially opening a case for in-cylinder reformation of ammonia.

Combustion

Observing the CoV of IMEPn data in Figure 17, it is evident that the presence of hydrogen has a positive impact on stability and combustion rate for all three combustion systems. For the SI system, the engine operates with excellent stability at 4 and 6 bar IMEPn compared to the pure ammonia operation points, with similar stability only observed at 12 bar IMEPn (reducing from 3% at the threshold load point of 8 bar IMEPn). For both MJI systems, the stability remains below 2%, peaking at 8bar IMEPn for both cases and reducing with increase in load similar to the SI system. Between both MJI systems passive JI show better stability than active JI due to the excess hydrogen in the fuel mix, as explained in the previous section and figures 5 and 6 both passive JI and SI tests were not conducted at the limit of combustion stability due to hydrogen injector having a higher minimum flowrate than required. As a result, the higher hydrogen content in the passive JI test result better stability than active JI which used a dedicated small flow injector.

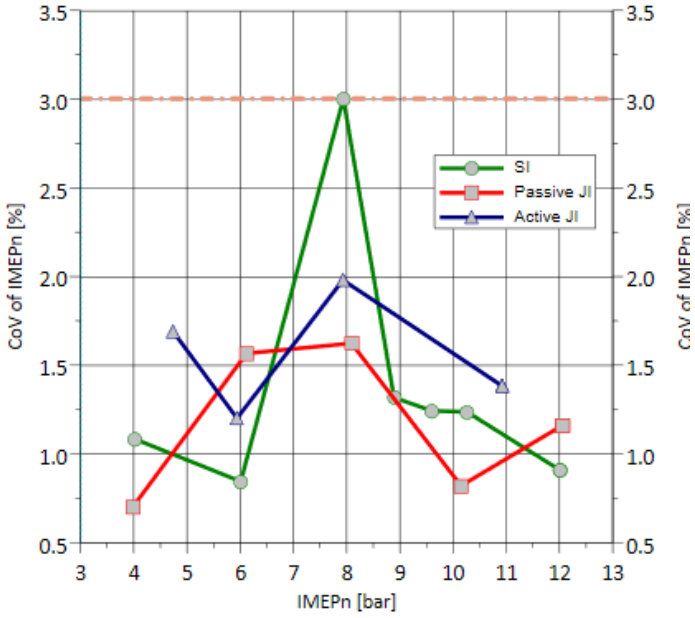

Figure 19 Stability of operation achieved by the combustion systems at various loads

Since the spark timing was targeting MBT (50% mass fraction burned, 8 CAD ATDC), combustion rate achieved by the various systems can be analysed by examining the spark timing data given in Figure 18. As expected, the presence of hydrogen increases the combustion rate. At low loads, both the active MJI and SI systems achieve better combustion rate than passive MJI (operating with less hydrogen than the latter). Between active MJI and SI, the distributed combustion of active MJI enables similar combustion to SI with ~5% less hydrogen energy fraction. This is much more evident at 11bar IMEPn, where SI systems require the spark to be advance by ~7 CAD in pure ammonia operation compared to active MJI which uses only 1% total hydrogen fraction concentrated in the pre-chamber.

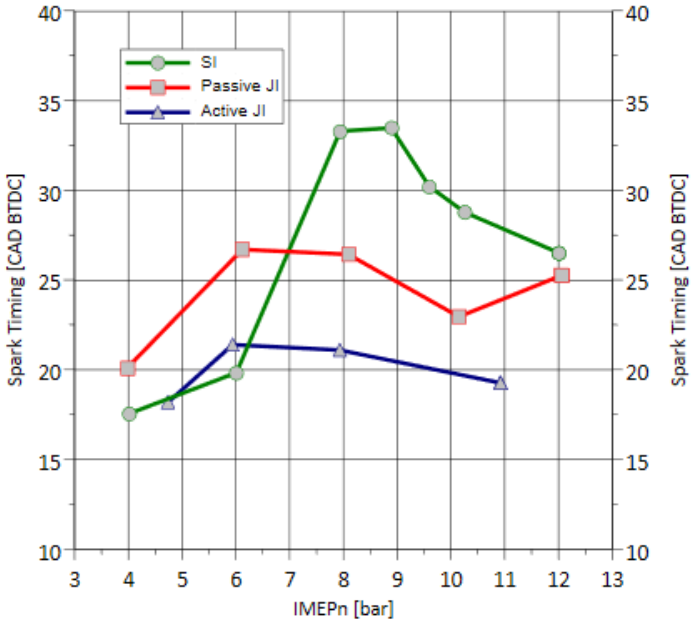

Figure 20 Spark advance need to achieve MBT spark timing at various load for the different combustion systems

Comparing both MJI ignition systems, even with higher hydrogen concentration in the passive MJI mode, the combustion rate is slower than active MJI, suggesting the potential higher energy fraction of ammonia in the pre-chamber hinders the combustion and jet formation for passive systems. This hypothesis can be further examined via the mass fraction burn data given data set out in Figures 19 and 20 respectively.

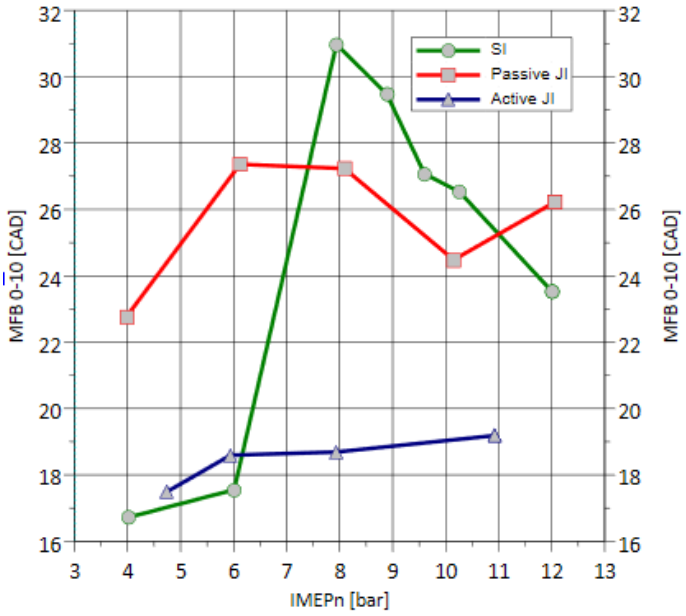

Figure 21 Variation of flame development phase (0-10% MFB) of the different combustion systems with engine load

As seen from the figure, having hydrogen in the fuel mix improves the flame development phase (0-10% MFB) for both active MJI and SI systems. The passive MJI system in comparison had a considerably longer flame development phasing owing to the diluted hydrogen concentration in the pre-chamber. Furthermore, analysing the hydrogen co-fuelling points with those of pure ammonia operation in SI, it is clear that the presence of hydrogen has a greater impact on the flame development phase than the combustion phase (10-90% MFB) as the duration of the development phase nearly doubles compared to the combustion phase the increase in duration is relatively small.

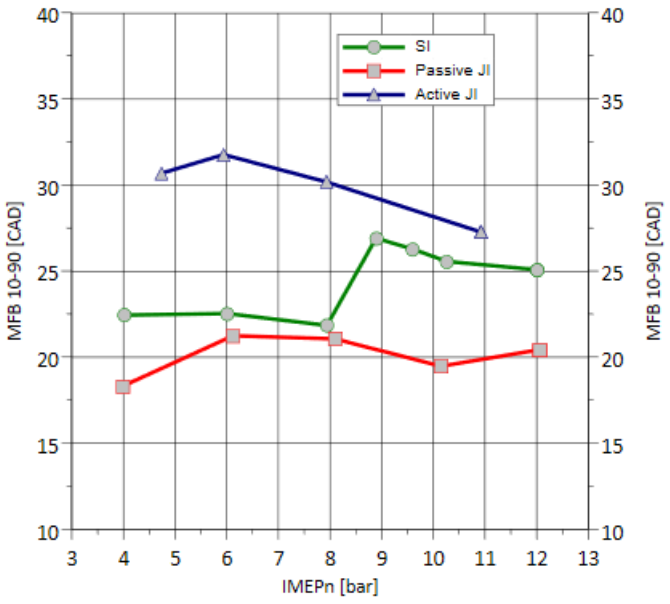

Figure 22 Variation of combustion phase (10-90% MFB) of the different combustion systems with engine load

Comparing the MJI systems, the passive variant exhibited a faster combustion phase than the active system, with the difference between them nearly the same as the flame development phase but in reverse (indicating the highly positive impact of hydrogen in the main chamber). This trend can be further investigated using the data of rate of heat release (RoHR) from the tests.

The plots for the various loads are illustrated in Figures 23-26.

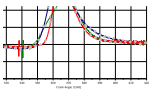

Figure 23 Variation of RoHR for the 3 combustion systems at 4bar IMEPn

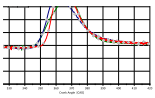

Figure 24 Variation of RoHR for the 3 combustion systems at 6bar IMEPn

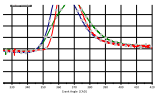

Figure 25 Variation of RoHR for the 3 combustion systems at 8bar IMEPn

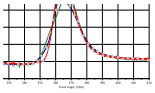

Figure 26 Variation of RoHR for the 3 combustion systems at 12bar IMEPn

As seen from all the figures, the RoHR of active MJI is peaks close to TDC at a magnitude lower than both SI and passive MJI tests. Furthermore, RoHR of active MJI tends to stagnate after TDC unlike passive MJI and SI where RoHR increases beyond TDC and falls immediately after the peak. This stagnation is the likely cause for increase MFB10-90 as the combustion of the fuel is delayed indicated by the gradual drop of RoHR compared to SI and passive MJI. Additionally the stagnation reduces with increase load showing a similar to MFB10-90, suggesting the phenomenon causing the stagnation of RoHR reduces with elevation in temperature and pressure.

The likely cause for this stagnation could be the quenching of flame front near the piston edge. In case of active MJI, most of the hydrogen is consumed within the pre-chamber resulting in the kinetics of the main chamber flame fully governed by the combustion characteristics of ammonia. Ammonia flame have significantly high quench distance compared to hydrogen and conventional fuels (Table 1) which tend to decrease at elevated temperatures and pressure [43] as observed with the trend in stagnation. Furthermore, the flame development in active MJI is significantly better increasing the likely hood of the flame front being close to the edge of the piston, where the distance between the cylinder head and piston is relatively small due to the pent roof design of the combustion chamber.

While a similar trend should be seen in passive MJI tests, this is likely due to the presence of hydrogen reducing the quench distance and a longer delay to the start of combustion both preventing the quenching of the flame front. In case of pure ammonia operation in SI, the likelihood of the flame being close to the piston edge is low due to the combustion initiating at the centre as opposed to the piston edge in case JI systems. Further tests are required to verify this hypothesis.

Emissions

The NOx and unburned ammonia data from the tests are given in Figures 27 and 28 respectively. The NOx emissions generally tended to reduce with increase in load, regardless of the presence of hydrogen, with the emissions from passive MJI system remaining nearly 100-200 ppm lower than SI for similar load conditions. Active MJI in comparison emits significantly lower NOx emissions, with the emissions remaining within 1000ppm for all load conditions. This results in ~60% reduction in NOx compared to SI at lower loads reducing to ~30% at the higher loads.

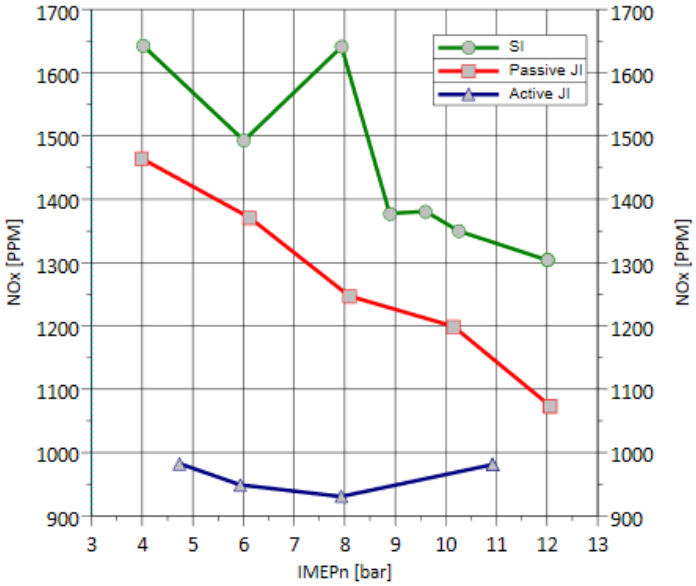

Figure 27 NOx emissions produced by the combustion systems at different engine loads

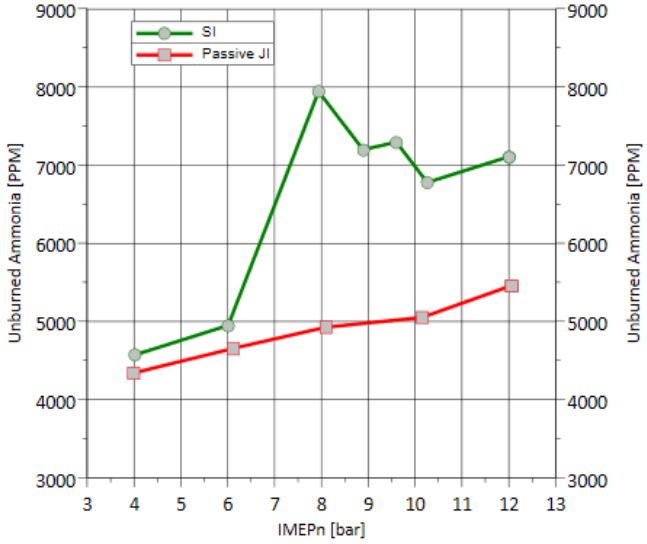

Figure 28 Unburned ammonia emission from SI and Passive MJI tests at various loads

Unburned ammonia in the exhaust also showed a similar trend, with the passive MJI system performing better than SI. However, the significant increase in unburned ammonia concentration for SI in pure ammonia operation (initially due to unstable operation) suggests that hydrogen present in the fuel mix could be the reason for low emissions in the MJI tests. This is further validated by comparable emissions in both cases at low loads with hydrogen co-fuelling, which in-turn suggests that the source of these emissions could be the ammonia trapped in the piston crevices. Ammonia has a significantly higher quench distance than hydrogen 22mm versus 0.9mm), and as a result combustion in the crevice region is less inhibited with the presence of hydrogen resulting in lower emissions of unburned ammonia. The unburned ammonia concentration for active MJI tests is not available for comparison due to the analyser being under maintenance during testing.

Conclusions

This report detailed experimental work undertaken to assess the feasibility of co-fuelling a modern SI engine with ammonia and hydrogen. The main findings were that engine could operate on well on pure ammonia at low speeds and moderate loads when the engine was fully warm, but it needed hydrogen to help it run stably at lower loads. The engine could use more than 70% ammonia at higher loads and speeds, and the spark timing could be optimized as the load increased. The combustion of pure ammonia had a long flame development phase that changed with load and speed, and a shorter combustion phase. The engine achieved a high thermal efficiency of 40% with pure ammonia at 1800rpm/16bar IMEPn, which could be improved further with higher loads and speeds. The NOx emissions were similar or lower with ammonia than with E10, while the ammonia slip emissions were high, especially at low loads, and could be reduced with hydrogen co-fuelling.

The viability of using MJI systems to burn ammonia-hydrogen mixtures was investigated by the comparing the results with that of SI combustion. Unlike SI systems, MJI systems are unable to operate on pure ammonia at any of the tested points requiring hydrogen for stable operation. The hydrogen demand reduces with load requiring as low as 1 % for 11 bar IMEPn in case of active MJI. Compared to SI, the combustion is faster for MJI systems in with the active having a better flame development phase and passive having a better combustion phase in the tests. The test also resulted in better emissions with MJI systems with lower NOx and unburned ammonia recorded in the MJI tests.

Active MJI systems shows significant promise as a combustion solution for ammonia engines. However detailed investigations are necessary to understand the impact of various parameters like pre-chamber design, air fuel composition etc on the operation of the engine. Immediate future work focusses on gaining a better understanding of the combustion with JI systems accompanied by detailed breakdown of NOx species (NO, N_2O, NO_2) at varied compression ratios and relative fuel to air ratios. The engine is also being modified to incorporate a longer stroke to bore ratio to enable operation with higher compression ratios that replicate the operation of a heavy-duty engine. In addition to this a single cylinder marine engine is being commissioned for further scalability tests with pre-chamber systems.

Acknowledgements

The authors would like to acknowledge the support of EPSRC in funding this research and Clean Air Power for their support in providing the ammonia and hydrogen injectors. The authors also would like to recognize the hard work and dedication of University of Nottingham's lab technicians to ensure the safety of all personnel in the Lab.

Reference List

1. IRENA, "A pathway to decarbonise the shipping sector by 2050," Abu Dhabi, ISBN 978-92-9260-330-4, 2021.

2. APC UK, "Thermal Propulsion Systems Roadmap 2020," 2021.

3. Korch Emerio, "Ammonia - A Fuel for Motor Buses," *Journal of Institute of Petroleum* 31:213–223, 1945.

4. Gray, J.T., Dimitroff, E., Meckel, N.T., and Quillian, R.D., "Ammonia Fuel — Engine Compatibility and Combustion," *SAE Transactions* 75:785–807, 1967.

5. Ryu, K., Zacharakis-Jutz, G.E., and Kong, S.C., "Performance characteristics of compression-ignition engine using high concentration of ammonia mixed with dimethyl ether," *Appl Energy* 113:488–499, 2014, doi:10.1016/J.APENERGY.2013.07.065.

6. Gross, C.W. and Kong, S.C., "Performance characteristics of a compression-ignition engine using direct-injection

ammonia–DME mixtures," *Fuel* 103:1069–1079, 2013, doi:10.1016/J.FUEL.2012.08.026.

7. Gill, S.S., Chatha, G.S., Tsolakis, A., Golunski, S.E., and York, A.P.E., "Assessing the effects of partially decarbonising a diesel engine by co-fuelling with dissociated ammonia," *Int J Hydrogen Energy* 37(7):6074–6083, 2012, doi:10.1016/J.IJHYDENE.2011.12.137.

8. Reiter, A.J. and Kong, S.C., "Combustion and emissions characteristics of compression-ignition engine using dual ammonia-diesel fuel," *Fuel* 90(1):87–97, 2011, doi:10.1016/J.FUEL.2010.07.055.

9. Reiter, A.J. and Kong, S.C., "Demonstration of compression-ignition engine combustion using ammonia in reducing greenhouse gas emissions," *Energy and Fuels* 22(5):2963–2971, 2008, doi:10.1021/EF800140F/ASSET/IMAGES/LARGE/EF-2008-00140F_0019.JPEG.

10. Pearsall, T.J. and Garabedian, C.G., "Combustion of Anhydrous Ammonia in Diesel Engines," *SAE Transactions* 76:3213–3221, 1968.

11. Pochet, M., Dias, V., Jeanmart, H., Verhelst, S., and Contino, F., "Multifuel CHP HCCI Engine towards Flexible Power-to-fuel: Numerical Study of Operating Range," *Energy Procedia* 105:1532–1538, 2017, doi:10.1016/J.EGYPRO.2017.03.468.

12. Tay, K.L., Yang, W., Li, J., Zhou, D., Yu, W., Zhao, F., Chou, S.K., and Mohan, B., "Numerical investigation on the combustion and emissions of a kerosene-diesel fueled compression ignition engine assisted by ammonia fumigation," *Appl Energy* 204:1476–1488, 2017, doi:10.1016/J.APENERGY.2017.03.100.

13. Starkman, E.S., Newhall, H.K., Sutton, R., Maguire, T., and Farbar, L., "Ammonia as a Spark Ignition Engine Fuel: Theory and Application," *SAE Transactions* 75:765–784, 1967.

14. Pyrc, M., Gruca, M., Tutak, W., and Jamrozik, A., "Assessment of the co-combustion process of ammonia with hydrogen in a research VCR piston engine," 2022, doi:10.1016/j.ijhydene.2022.10.152.

15. Xin, G., Ji, C., Wang, S., Meng, H., Chang, K., and Yang, J., "Effect of ammonia addition on combustion and emission characteristics of hydrogen-fueled engine under lean-burn condition," *Int J Hydrogen Energy* 47(16):9762–9774, 2022, doi:10.1016/J.IJHYDENE.2022.01.027.

16. Dinesh, M.H. and Kumar, G.N., "Effects of compression and mixing ratio on NH 3 /H 2 fueled Si engine performance, combustion stability, and emission," *Energy Conversion and Management : X* 15:100269, 2022, doi:10.1016/j.ecmx.2022.100269.

17. Hong, C., Ji, C., Wang, S., Xin, G., Qiang, Y., and Yang, J., "Evaluation of hydrogen injection and oxygen enrichment strategies in an ammonia-hydrogen dual-fuel engine under high compression ratio," *Fuel* 354:129244, 2023, doi:10.1016/J.FUEL.2023.129244.

18. Wang, Y., Zhou, X., and Liu, L., "Theoretical investigation of the combustion performance of ammonia/hydrogen mixtures on a marine diesel engine," 2021, doi:10.1016/j.ijhydene.2021.01.233.

19. Mercier, A., Mounaïm-Rousselle, C., Brequigny, P., Bouriot, J., and Dumand, C., "Improvement of SI engine combustion with ammonia as fuel: Effect of ammonia dissociation prior to combustion," *Fuel Communications* 11:100058, 2022, doi:10.1016/J.JFUECO.2022.100058.

20. Comotti, M. and Frigo, S., "Hydrogen generation system for ammoniae hydrogen fuelled internal combustion engines," 2015, doi:10.1016/j.ijhydene.2015.06.080.

21. Mørch, C.S., Bjerre, A., Gøttrup, M.P., Sorenson, S.C., and Schramm, J., "Ammonia/hydrogen mixtures in an SI-engine: Engine performance and analysis of a proposed fuel system," *Fuel* 90(2):854–864, 2011, doi:10.1016/J.FUEL.2010.09.042.

22. Frigo, S. and Gentili, R., "Analysis of the behaviour of a 4-stroke Si engine fuelled with ammonia and hydrogen," *Int J Hydrogen Energy* 38(3):1607–1615, 2013, doi:10.1016/J.IJHYDENE.2012.10.114.

23. Frigo, S., Gentili, R., and Angelis, F. De, "Further insight into the possibility to fuel a SI engine with ammonia plus hydrogen," *SAE Technical Papers* 2014, 2014, doi:10.4271/2014-32-0082.

24. Lhuillier, C., Bréquigny, P., Contino, F., and Mounaïm-Rousselle, C., "EXPERIMENTAL STUDY ON NH3/H2/AIR COMBUSTION IN SPARK-IGNITION ENGINE CONDITIONS," *Fuel* 269, 2020, doi:https://doi.org/10.1016/j.fuel.2020.117448.

25. Mounaïm-Rousselle, C., Mercier, A., Brequigny, P., Dumand, C., Bouriot, J., Houillé, S., and Mounaı̈m-Rousselle, C.M., "Ignition engine," *Interna-Tional Journal of Engine Research* 146808742110387, 2021, doi:10.1177/14680874211038726ï.

26. Grove, J.R., "THE MEASUREMENT OF QUENCHING DIAMETERS AND THEIR RELATION TO THE FLAMEPROOF GROUPING OF GASES AND VAPOURS," *Institute of Chemical Engineers* 25, 1968.

27. Dimitriou, P. and Javaid, R., "A review of ammonia as a compression ignition engine fuel," *Int J Hydrogen Energy* 45(11):7098–7118, 2020, doi:10.1016/J.IJHYDENE.2019.12.209.

28. Lhuillier, C., Brequigny, P., Contino, F., and Rousselle, C., "Combustion Characteristics of Ammonia in a Modern Spark-Ignition Engine," *SAE Technical Papers* (October), 2019, doi:10.4271/2019-24-0237.

29. Robinson, A.P.L., Strozzi, D.J., Davies, J.R., Kumamoto, A., Iseki, H., Ono, R., and Oda, T., "Conference Series OPEN ACCESS To cite this article: Ayumi Kumamoto et al," *J. Phys.: Conf. Ser* 301:12039, 2011, doi:10.1088/1742-6596/301/1/012039.

30. Ciniviz, M. and Köse, H., "Academic @ Paper HYDROGEN USE IN INTERNAL COMBUSTION ENGINE: A REVIEW," *International Journal of Automotive Engineering and Technologies* 1:1–15, 2012.

31. Hamori, F., Harry, P., and Watson, C., "Hydrogen Assisted Jet Ignition for the Hydrogen Fuelled SI Engine," *World Hydrogen Energy Conference* , 2006.

32. Dober G.G and Watson H.C, "Modelling the flame enhancement of a HAJI equipped spark ignition engine. ipc-10-99/ipc99091 - FISITA," https://go.fisita.com/store/papers/ipc-10-

99/ipc99091?search=53616c7465645f5f3ea0803fe28c987220fc5598390c4c3e54bdd77d07e65286bd9e5d8b4b976a1d308303cdc4bae2772d23c7e0dd613478f6034b0042e4263d81bee1245d4e4954c359c5b5bcef59e056be1bbed1ac1f964c51f844312f3df7b6293a90ce3e5d27325cf060708cc8deb7714e1aa2e66b2fe49933c44c7cd9403746f094aab1a54b, 1999.

33. Boretti, A.A. and Watson, H.C., "The lean burn direct injection jet ignition gas engine," *Int J Hydrogen Energy* 34(18):7835–7841, 2009, doi:10.1016/J.IJHYDENE.2009.07.022.

34. Css K We Sn, N.S. and st HB, S.N., "Internal combustion engine ignition device," *Sheet* 1(6):307, 1992.

35. Wang, Y., Zhou, X., and Liu, L., "Feasibility study of hydrogen jet flame ignition of ammonia fuel in marine low speed engine," *Int J Hydrogen Energy* 48(1):327–336, 2023, doi:10.1016/j.ijhydene.2022.09.198.

36. Cui, Z., Tian, J., Zhang, X., Yin, S., Long, W., and Song, H., "Experimental Study of the Effects of Pre-Chamber Geometry on the Combustion Characteristics of an Ammonia/Air Pre-Mixture Ignited by a Jet Flame," *Processes 2022, Vol. 10, Page 2102* 10(10):2102, 2022, doi:10.3390/PR10102102.

37. Zhang, X., Tian, J., Cui, Z., Xiong, S., Yin, S., Wang, Q., and Long, W., "Visualization study on the effects of pre-chamber jet ignition and methane addition on the combustion characteristics of ammonia/air mixtures," *Fuel* 338:127204, 2023, doi:10.1016/J.FUEL.2022.127204.

38. Hancock, D., Fraser, N., Jeremy, M., Sykes, R., and Blaxill, H., "A new 3 cylinder 1.2l advanced downsizing technology demonstrator engine," *SAE Technical Papers*, 2008, doi:10.4271/2008-01-0611.

39. Kobayashi, H., Hayakawa, A., Somarathne, K.D.K.A., and Okafor, E.C., "Science and technology of ammonia combustion," *Proceedings of the Combustion Institute* 37(1):109–133, 2019, doi:10.1016/J.PROCI.2018.09.029.

40. Silva, M., Almatrafi, F., Uddeen, K., Cenker, E., Sim, J., Younes, M., Jamal, A., Guiberti, T., Turner, J., and Im, H., "Computational Assessment of Ammonia as a Fuel for Light-Duty SI Engines," *SAE Technical Papers*, 2023, doi:10.4271/2023-24-0013.

41. Mounaïm-Rousselle, C., Bréquigny, P., Dumand, C., and Houillé, S., "Operating Limits for Ammonia Fuel Spark-Ignition Engine," *MDPI*, 2021, doi:10.3390/en14144141.

42. Girard, J., Snow, R., Cavataio, G., and Lambert, C., "The influence of ammonia to NOX ratio on SCR performance," *SAE Technical Papers*, 2007, doi:10.4271/2007-01-1581.

43. Takizawa, K., Igarashi, N., Tokuhashi, K., and Kondo, S., "Effects of temperature and pressure on quenching distances of difluoromethane (R32) and ammonia (R717)," *Sci Technol Built Environ* 24(1):97–104, 2018, doi:10.1080/23744731.2017.1328941.

Contact

Ajith Ambalakatte.
Powertrain Research Centre
Faculty of Engineering
University of Nottingham
University Park.
Nottingham, UK
NG7 2RD
Email : ajith.amblakatte1@nottingham.ac.uk

Sikai Geng
Powertrain Research Centre
Faculty of Engineering
University of Nottingham
University Park.
Nottingham, UK
NG7 2RD
Email : sikai.geng@nottingham.ac.uk

Jonathan Hall
Head of Research & Advanced Engineering
MAHLE Powertrain Ltd
Costin House
St James Mill Road
Northampton, UK
NN5 5TZ
Email : jonathan.hall@mahle.com

DefInitions

CAD : Crank Angle Degree
NH_3 : Ammonia
NOx : Oxides of Nitrogen
SI : Spark Ignition
LHV : Lower Heating Value
ITE : Indicated Thermal Efficiency
MFB : Mass Fraction Burned
CoV : Coefficient of Variance
E10 : Gasoline with 10% Ethanol
CI : Compressed Ignition
DI: Direct injection
PFI : Port Fuel Injection
BTDC : Before Top Dead Centre
BTDCf : Before Top Dead Centre firing
MBT: Maximum Brake Torque
ppm : Parts Per Million
IMEPn : Net Indicated Mean Effective Pressure